Journal of Oceanology and Limnology
Vol. 42, No. 3, pp. 772-786, 2024
https://doi.org/10.1007/s00343-023-2372-6

Research Paper

Biogeochemistry of sedimentary organic matter in the Yongjiang River estuary in the southern part of Hangzhou Bay, China, since the Late Pleistocene*

Dongqin HUANG[1], Xiaolong LI[1, 2], Zilong LI[1, **], Pei Sun LOH[1, **], Jianxiong HU[1], Jianfang CHEN[3], Yuan-Pin CHANG[4], Chin-Wen YANG[4], Qin GAO[1]

[1] *Institute of Marine Geology and Resources, Ocean College, Zhejiang University, Zhoushan 316021, China*

[2] *Ministry of Water Resources of the People's Republic of China, Beijing 100054, China*

[3] *Key Laboratory of Marine Ecosystem Dynamics, Second Institute of Oceanography, Ministry of Natural Resources, Hangzhou 310012, China*

[4] *Department of Oceanography, Sun Yat-sen University, Kaohsiung 80424, China*

Received Nov. 21, 2022; accepted in principle Mar. 8, 2023; accepted for publication Jul. 20, 2023

Abstract A sediment core (YJK19-02) collected from the southern outlet of Hangzhou Bay near the Yongjiang River estuary in East China was analyzed for grain size, lignin, bulk elemental composition, stable carbon isotope, and rare earth elements (REEs) to determine the sources and diagenesis of sedimentary organic matter (OM) of the estuary and adjacent areas since the Late Pleistocene. $\delta^{13}C$ values (-24.80‰–-23.60‰), total organic carbon/total nitrogen (TOC/TN) molar ratios (8.00–12.14), and light rare earth element/heavy rare earth element ratios (LREE/HREE=8.34–8.91) revealed the predominance of terrestrial sources of OM, mainly from the Changjiang (Yangtze) River. The lignin parameters of syringyl/vanillyl (S/V=0.20–0.73) and cinnamyl/vanillyl (C/V=0.03–0.19) ratios indicate the predominance of nonwoody angiosperms, and the vanillic acid/vanillin ratios [$(Ad/Al)_V$=0.32–1.57] indicate medium to high degrees of lignin degradation. An increasing trend of Λ (total lignin in mg/100-mg OC) values from ca. 14 500 a BP to ca. 11 000 a BP reflected the increase in temperature during the Late Pleistocene. However, a time lag effect of temperature on vegetation abundance was also revealed. The relatively higher and stable Λ values correspond to the higher temperature during the mid-Holocene from ca. 8 500 a BP to ca. 4 500 a BP. Λ values decreased from ca. 4 000 a BP to the present, corresponding to historical temperature fluctuations during this time. Our results show that the vegetation abundance in the Yongjiang River Basin since the Late Pleistocene was related to the temperature fluctuation duo to climate change.

Keyword: Yongjiang River estuary; sedimentary organic matter; lignin; environmental change; Late Pleistocene

1 INTRODUCTION

Estuaries and shelf seas account for only 10% of the total sea-floor area but are composed of more than 90% of ocean sedimentary organic matter (OM) due to high input from land and primary productivity (Hedges et al., 1997; Xing et al., 2011). Therefore, studies of OM composition and evolution are critical for understanding the global carbon cycle (Tesi et al., 2007; Zhang et al., 2015). Many scholars have used different methods to trace the biogeochemistry of sedimentary OM in coastal zones, including element and isotope geochemistry and biological indicators (Zhang et al., 2007; Wang et al., 2015; Yang et al., 2021). Because lignin has been found exclusively in terrestrial vascular plants, lignin has been widely used as a biomarker to terrestrial OM (Hedges and Mann, 1979; Orem et al.,

* Supported by the China Institute of Water Resources and Hydropower Research (No. K20231586), the Water Conservancy Bureau of Yunyang County (No. YYX24C00008), the Ecological Forestry Development Center of Lishui City (No. 2021ZDZX03), and the Asia-Pacific Network for Global Change Research (No. CRRP2020-06MY-Loh)

** Corresponding authors: zilongli@zju.edu.cn; psloh@zju.edu.cn

1997; Zhang et al., 2013), aiding in the identification and reconstruction of the origin, transportation, and distribution of terrestrial OM in various nearshore environments (Loh et al., 2008; Tareq et al., 2011; Jex et al., 2014; Gong et al., 2017). There are three groups of lignin index phenols: vanillyl (V), syringyl (S), and cinnamyl (C). Only vascular plants generate V-based phenols (Hedges and Mann, 1979; Goñi and Hedges, 1992), while S phenols are produced mainly by angiosperms (Hedges and Mann, 1979), and nonwoody tissues yield higher C phenols than woody tissues (Hedges and Parker, 1976; Hu et al., 1999). Hence, the compositions of the three phenol groups can be used to distinguish woody from nonwoody plant types and angiosperm from gymnosperm tissues (Goñi et al., 2000; Tareq et al., 2011; Winterfeld et al., 2015). Other parameters (stable carbon isotope, total organic carbon/total nitrogen (TOC/TN), and rare earth elements (REEs)) have been often used together with lignin to identify OM sources (Onstad et al., 2000; Liu et al., 2015; Yang et al., 2021).

The Changjiang (Yangtze) River estuary, Hangzhou Bay, and the adjacent areas along the eastern coast of China are zones with strong interactions between the land and the ocean. These coastal areas have special geological structures, complex and diversified hydrodynamic conditions, and sediments that are vulnerable to strong tidal and coastal currents (Zhang et al., 2013). Therefore, many studies have been carried out to determine the past environmental changes of these coastal areas. Reconstruction of the past climate along the Chinese coast has been carried out in the Hangzhou Bay (Liu et al., 2018b, 2020), the Changjiang River estuary (Wang and Yang, 2013; Wang et al., 2018), and the East China Sea (Kawahata and Ohshima, 2004; Chang et al., 2009). Wang et al. (2018) collected sediment cores to study the three-dimensional evolution of the Changjiang River mouth during the Holocene, and Li et al. (2016) collected a sediment core from the East China Sea and used bulk parameters and lignin to analyze sediment sources and reconstruct regional paleoclimate changes and human disturbances. Previous studies on the sediments in Hangzhou Bay and the Yongjiang River estuary focused primarily on shallow surface sediments (Kuai et al., 2017; Li et al., 2018; Zhao et al., 2018c; Song et al., 2020). Zhang et al. (2015) analyzed the grain size composition and transport of sedimentary OC in surface sediments in the Changjiang River estuary and Hangzhou Bay and their adjacent waters, and Kuai et al. (2017) studied the sources and transport mechanisms of surface sediments at the Yongjiang River estuary. Similarly, Song et al. (2020) studied the transport mechanisms of suspended sediments and the migration trends of sediments in the central Hangzhou Bay. However, while many studies have been done in this area, relatively few have focused on the sediments of the Yongjiang River estuary in the southern outlet of Hangzhou Bay. Thus, for this study, a sediment core was collected from the southern outlet of Hangzhou Bay near the Yongjiang River and analyzed for vertical distribution characteristics, including ^{14}C age, grain size, bulk elemental composition, stable carbon isotopes, lignin-derived phenols, and REEs. The objective of this study was to determine the sources and diagenesis of sedimentary OM at the Yongjiang River estuary since the Late Pleistocene, and to provide a foundation for further studies of the sediment and environmental changes in the Changjiang River, Hangzhou Bay, and adjacent coastal areas.

2 MATERIAL AND METHOD

2.1 Study area and sampling

Hangzhou Bay is a funnel-shaped estuary located in the northern part of Zhejiang Province adjacent to the East China Sea. The bay can be divided into inner and outer bays (Pang et al., 2017). Covering an area of approximately 8 500 km^2, it is one of the world's largest macro tidal bays (Zhu et al., 2018) and has a wide tidal range and strong tidal currents (Chen et al., 2019). The sediment sources of Hangzhou Bay are complex and diverse. In addition to the materials input from the Changjiang River, the bay also receives materials from the Qiantang River and other surrounding rivers. Its sedimentation rate is greatly affected by the Changjiang River (Xie et al., 2017). The sediments in Hangzhou Bay are mainly silt and clay (Su and Wang, 1989).

The Yongjiang River is situated in the eastern Zhejiang Province of China and discharges into the southern outlet of Hangzhou Bay. The total length of the Yongjiang River is 130 km, with a basin area of 4 572 km^2. It is formed by the convergence of the Fenghua River and Yaohe River and flows from southwest to northeast. The Yongjiang River estuary is bell shaped and has an obvious tidal phenomenon. The sediments of the Yongjiang River estuary are mainly from the Changjiang River estuary and are composed of clayey silt sediments (Kuai et al., 2017). Both the Yongjiang River estuary and

Hangzhou Bay are affected by tidal action, and the strong tidal current is the main driving force of sediment transport and deposition in this area, followed by waves (Su and Wang, 1989). Materials from the Changjiang River, with input from the Qiantang River and Hangzhou Bay, flow out of the bay and pass through the Yongjiang River estuary. Thus, the historical signature of the Yongjiang River estuary will likely reflect changes in the Changjiang River, Hangzhou Bay, and the adjacent coastal areas.

A sediment core of about 9 m long was collected near the Yongjiang River estuary (29°58′40″N, 121°46′40″E; Fig.1) in June 2019 using a borehole corer. Sediment samples were sliced and stored in a sealed plastic bag in darkness. In the laboratory, they were stored frozen for later analysis. A 2-cm thick sediment sample was taken from each of the nine depths (0.6, 1.6, 2.6, 3.6, 4.6, 5.6, 6.6, 7.6, and 8.6 m) for grain size and REE analyses, and a 2-cm thick sediment sample was taken from each of 18 depths (0.6, 0.9, 1.6, 1.9, 2.6, 2.9, 3.6, 3.9, 4.6, 4.9, 5.6, 5.9, 6.6, 6.9, 7.6, 7.9, 8.6, and 8.9 m) for bulk elemental, stable isotope, and lignin analyses.

2.2 AMS ^{14}C dating

The sediment samples were dried in an oven at 45 °C and then dispersed in clear water. Shells, foraminifera, and other plant fragments were screened. Three sediment samples were analyzed to obtain three effective ages at 0.6-, 3.6-, and 6.6-m depths; the sediments were dated using plant fragments from samples at 0.6-m and 6.6-m depths and foraminifera from 3.6-m sample. AMS ^{14}C dating was executed using an accelerator mass spectrometer (AMS) HVE 1.0 MV Tandetron Model 4110 BO (High Voltage Engineering Europa B.V., Netherlands). Dates between 50 000 BP and 1 BP were calibrated using the calibration curve IntCal13. All ratio measurements have 2σ uncertainty. The ages of the sediments were expressed as calendar ages (cal. a BP, before 1950 CE). The age model used in the present study is based on linear interpolations of ^{14}C ages.

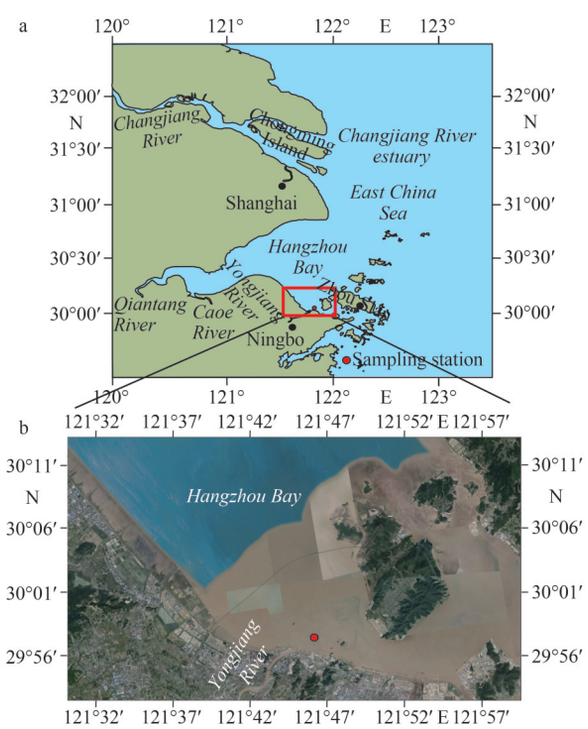

Fig.1 Geographic location of the study area (a) and sampling location of the sediment core in the Yongjiang River estuary (b)

2.3 Lignin analysis

Lignin-derived oxidation products were extracted using the alkaline cupric oxide oxidation method defined by Hedges et al. (1982). Approximately 0.5 g of dried sediment samples and 1.0 g of CuO powder in PTFE vessels were oxidized under basic conditions (10-mL 2-mol/L NaOH) in an oxygen-free atmosphere by heating in a muffle furnace at 150 °C in 3 h and shaken hourly. After the oxidation process, the contents of the vessel were centrifuged three times for 10 min at 2 000 r/min. After centrifugation, the supernatant was acidified to pH 1 by adding 6-mol/L HCl. Acidified supernatant was extracted three times with 10-mL ethyl acetate, dried with anhydrous Na_2SO_4, and then 100-μL ethyl vanillin was added as an internal standard. The solution was then evaporated using a rotary evaporator until it was nearly dry and then transferred into a vial where it was blown with N_2 until it was completely dry. Subsequently, 100-μL pyridine and 100-μL bis-(trimethylsilyl) trifluoroacetamide with 10% trimethylchlorosilane (BSTFA+10%, TMCS) were added to the vial, and the sample was derivatized at 90 °C for 10 min. After the derivatization process, the solution was analyzed using gas chromatography (GC) with flame ionization detection 2010 Plus (Shimadzu, Japan). The column temperature was programmed to increase from 100 °C to 300 °C at a rate of 4 °C/min and then stayed at 270 °C. The yields of lignin phenol compounds were calculated using the response factors of injected mixtures of commercial standard compounds. Thus, the properties of each lignin phenol were determined based on the retention time of the standards, and the peak area of

each lignin phenol was compared with the peak area of the internal standard to determine the lignin phenol concentrations of each sample.

2.4 Bulk elemental and stable isotope analysis

The sediments were acidified with 1-mol/L HCl solution to remove the inorganic carbon. Subsequently, the sediments were dried in an oven at 45 °C and then homogenized using a mortar and pestle. Precisely 20 mg of dry sediments were placed onto a 4-mm×4-mm×11-mm piece of tin foil that was then folded into a pellet. The total organic carbon (TOC) and total nitrogen (TN) contents of the samples were determined using a Vario ISOTOPE cube elemental analyzer (Elementar, Germany). The standard reference material used was sulfanilamide, and the accuracy for TOC and TN was 0.02% and 0.005%, respectively. All C/N ratios were calculated as TOC/TN molar ratios.

The acid-treated samples underwent carbon isotope analysis using an elemental analyzer, isotope ratio mass spectrometry (Delta V Advantage, Thermofisher Scientific, Germany). The analytical results were calibrated using international standard V-PDB (Boutton, 1991) as follows:

$$\delta\ (‰)=(R_{sample}/R_{standard}-1)\times 1000,$$

where δ (‰) represents the isotopic ratio of the tested sample, R_{sample} refers to the $^{13}C/^{12}C$ ratio of the sample, and $R_{standard}$ refers to the $^{13}C/^{12}C$ ratio of the standard sample. An IAEA-CH_3 standard substance ($\delta^{13}C$=-24.72‰) was subjected to stable carbon isotope measurement every 10 samples, and the relative standard deviation of the IAEA-CH_3 standard was <0.2‰.

2.5 Grain size analysis

For grain size analysis, sediment samples weighing approximately 20 mg were taken. H_2O_2 was added to remove OM, and HCl was used to remove carbonate, followed by washing and centrifuging the sediment. Subsequently, grain size was determined using a BT-2002 laser particle size analyzer (Dandong Baxter, China). The deviations of the measured values were usually smaller than 3%.

2.6 Rare earth element analysis

The sediment samples were dried in an oven at 45 °C and ground to below 200 mesh using a mortar and pestle. Approximately 1 g of sediment sample was digested with HNO_3 and HF solution in a Teflon vessel and then extracted and separated; REEs were determined using a Thermo Fisher quadrupole inductively coupled plasma mass spectrometer (ICP-MS; Germany). The deviations of the measured values were usually smaller than 5%.

3 RESULT

3.1 Sediment age and grain size

The sample ages were obtained through AMS ^{14}C dating (Supplementary Table S1). After excluding anomalous data and assuming a constant rate of sedimentation between the obtained dates, sedimentation rates were obtained through linear interpolation of the calibrated ages along the sediment core (Fig.2), thus enabling the calculation of the age of the remaining sediment samples and the construction of an age vs. depth model. The model revealed that the core spanned ca. 14.5 cal ka BP, with a sedimentation rate a range of 0.016 9–0.017 4 cm/a.

The median diameter of the grain size along the core ranged from 9.30 to 41.31 μm, on average of 23.42 μm. The contents of the sand (0.063–2 mm), silt (0.003 9–0.063 mm), and clay (<0.003 9 mm) at different depths were obtained using the classification and naming method proposed by Folk et al. (1970). In general, grain sizes along the core decreased gradually from 33.93 μm at 8.9 m (ca. 14 500 a BP) to 11.90 μm at 6.9 m (ca. 11 000 a BP), then increased to a maximum value of 41.31 μm at 3.9 m (ca. 5 770 a BP), and decreased to 9.30 μm at 0.9 m (ca. 7 520 a BP; Fig.2).

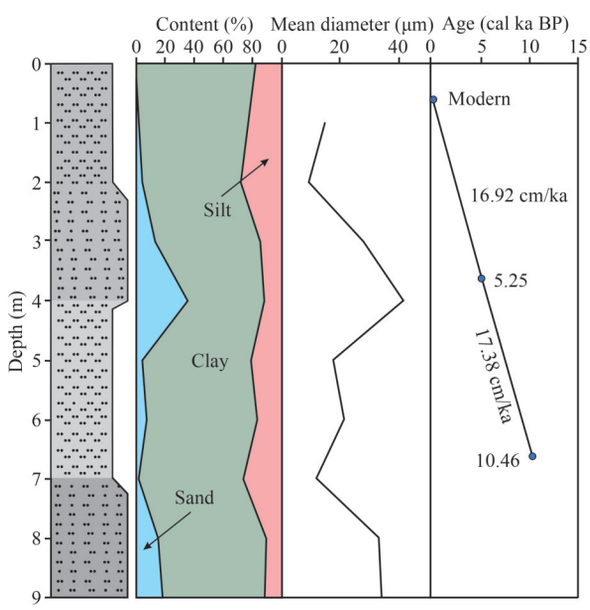

Fig.2 Lithology and chronology of the core YJK19-02 in the Yongjiang River estuary

3.2 TOC, TN, C/N ratio, and $\delta^{13}C$ value

The bulk elemental (TOC, TN, and C/N) and stable carbon isotope compositions ($\delta^{13}C$) of the sediment core were compiled according to their depths and ages (Supplementary Table S2; Fig.3). TOC percentages ranged from 0.27% to 0.68% on average of 0.55%±0.10%. TN percentages ranged from 0.03% to 0.09%, on average of 0.06%±0.01% (n=18). The overall trend of both the TOC and TN was a decrease from 8.9 to 6.9 m, an increase at 6.6 m, and then a decrease to 3.9 m where the minimum value was reached. The vertical variation trend of TOC and TN values was similar. In general, the TOC and TN values decreased from 8.9 to 3.9 m and reached a minimum value of 3.9 m (TOC= 0.27% and TN=0.03%, respectively). Subsequently, TOC and TN values showed a decreasing trend from 3.9 to 0.6 m and a gradual increase from 3.9 to 0.6 m (from ca. 5 770 a BP to 169 a BP).

The values of TOC/TN molar ratios ranged from 8.00 to 12.14 on average of 10.27±1.11 (n=18) throughout the entire core. The TOC/TN ratios were higher at the bottom of the core and decreased toward the surface sediments, which indicates a decrease in terrestrial OM from 8.9 to 3.9 m and a reduction in terrestrial OM toward the present (Fig.3). The $\delta^{13}C$ values ranged from -24.80‰ to -23.60‰ along the core, with a mean of -23.41‰ ±0.33‰. They were more negative at the bottom than at the top of the core, and the most negative value of -24.74‰ was found at 5.6 m. The trends of TOC/TN and $\delta^{13}C$ were roughly the same, both indicating an increase in marine OM and a decrease in terrestrial OM toward the surface (Fig.3).

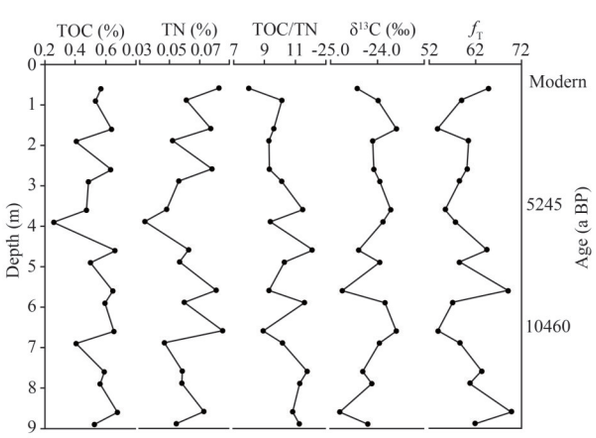

Fig.3 Vertical distribution of TOC, TN, TOC/TN, and $\delta^{13}C$ values along the length of the sediment core in the Yongjiang River estuary

3.3 Lignin oxidation product

The changes in lignin parameters along the sediment core of the Yongjiang River estuary are presented in the Supplementary Table S3 and Fig.4. The Λ values of the sediment core samples ranged from 0.93 to 3.09 (total lignin in mg/100-mg OC), with an average value of 2.02. The overall Λ values tended to increase gradually from 1.70 at 8.9 m to 3.09 at 6.9 m and then showed an overall trend of gradual decrease from 3.09 at 6.9 m to 2.28 at 0.6 m.

The syringyl/vanillyl (S/V) and cinnamyl/vanillyl (C/V) ratios were used to distinguish vegetation types, as the S/V values of gymnosperms and angiosperms are very low (S/V≈0) and relatively high (S/V>0.6), respectively, and the C/V values were used to distinguish between woody (C/V<0.1) and nonwoody (C/V>0.1) plant tissues (Hedges and Mann, 1979; Goñi et al., 2000). The S/V values ranged from 0.20 to 0.73, with an average value of 0.46±0.14 (n=18), and the C/V ratios ranged from 0.03 to 0.19, with an average value of 0.09±0.04 (n= 18), indicating the presence of woody and nonwoody angiosperms in the Yongjiang River estuary. The overall trend of S/V values was a gradual increase from 0.29 at 8.9 m to 0.72 at 6.9 m, followed by a decrease to 0.42 at 0.6 m with a high S/V of 0.73 observed at 2.9 m. The C/V values showed an increasing trend from 0.08 at 8.9 m to 0.19 at 6.9 m, and a maximum value of 0.19±0.04 was found at 6.9 m. Subsequently, the C/V values decreased gradually to 0.06 at 0.6 m. The C/V ratios showed the same trend as the S/V ratios (Fig.4).

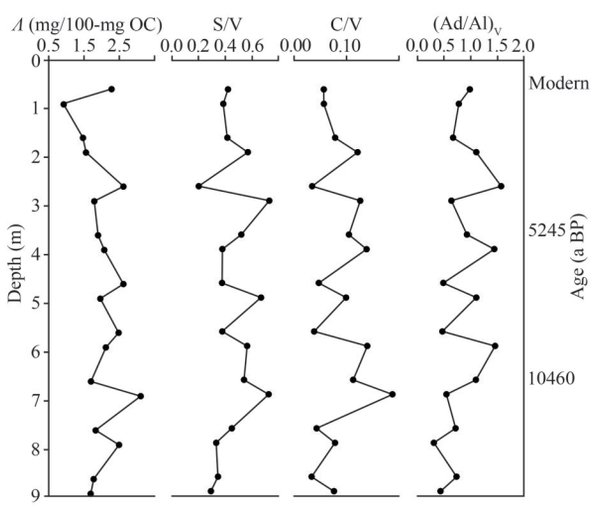

Fig.4 Vertical distribution of lignin oxidation products along the length of the sediment core in the Yongjiang River estuary

The vanillic acid/vanillin ratio or $(Ad/Al)_V$ is an indicator of the degree of oxidative degradation of lignin. $(Ad/Al)_V$ values between 0 and 0.3 indicate fresh plant tissue, $(Ad/Al)_V$ values of 0.3 to 0.5 indicate that the lignin has undergone moderate degradation, while $(Ad/Al)_V$ values above 0.5 indicate frequent microbial activity and a high degree of lignin degradation (Hedges and Parker, 1976). The $(Ad/Al)_V$ values of the Yongjiang River estuary core ranged from 0.32 to 1.57, with an average value of 0.86±0.36 (n=18), indicating that most lignin had undergone medium to high degradation (Hedges and Parker, 1976). Generally, the $(Ad/Al)_V$ values showed an upward trend from the bottom to top with a decrease from 2.6 to 0.6 m (Fig.4).

3.4 Characteristic of rare earth elements

Variations in total rare earth elements (ΣREEs) abundances along the sediment core are shown in the Supplementary Table S4 and Fig.5. The REEs include LREE (La, Ce, Pr, Nd, Sm, and Eu) and HREE (Gd, Tb, Dy, Ho, Er, Tm, Yb, and Lu). The ΣREEs along the sediment core ranged from 182.26 to 209.38 μg/g, with an average of 195.08 μg/g. The contents of LREE ranged from 163.45 to 188.26 μg/g, with an average of 174.90 μg/g. The contents of HREE were between 18.73 and 21.26 μg/g, with an average of 20.18 μg/g, which was far smaller than the content of LREE. The LREE/HREE ratios ranged from 8.34 to 8.91, with an average value of 8.66, reflecting good differentiation between LREE and HREE (Minai et al., 1992; Jung et al., 2021). And the values of ΣLREE, ΣHREE, ΣREE, LREE/HREE had the same overall trend of changes from 5.9 m to the present along the length of the core.

4 DISCUSSION

4.1 Sedimentary environment dynamic

Environmental conditions can be inferred based on the compositional changes in granularity (McLaren and Bowles, 1985). Sand is generally a moving component, indicating strong to medium hydrodynamic conditions, while silt and clay are mostly suspended components, reflecting low to medium environmental energy. Hence, coarser particles reflect a high-energy and unstable sedimentary environment with stronger hydrodynamic conditions, while fine sediments indicate a low-energy and more stable sedimentary environment with weak hydrodynamic sorting (Wan et al., 2007). The grain sizes of the sediments along the core at the Yongjing River estuary ranged from 9.30 to 41.31 μm, indicating the presence of mostly fine sediment. Our results are consistent with previous findings in which the grain sizes of sediments in southeastern China were determined to be relatively fine and composed mainly of clay and silt, indicating that these sediments were formed in a low-energy and stable sedimentary environment (Liu et al., 2018a; Zhao et al., 2018c).

Pejrup (1988) proposed a triangular graphic method to distinguish an estuarine sedimentary environment that uses the structural composition of sediments to represent the hydrodynamic strength of the water, as shown in Fig.6. The content of sand

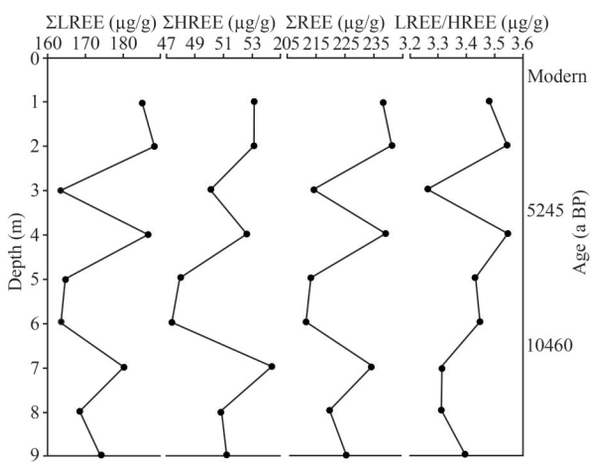

Fig.5 Vertical distribution of the trace elements along the length of the sediment core in the Yongjiang River estuary

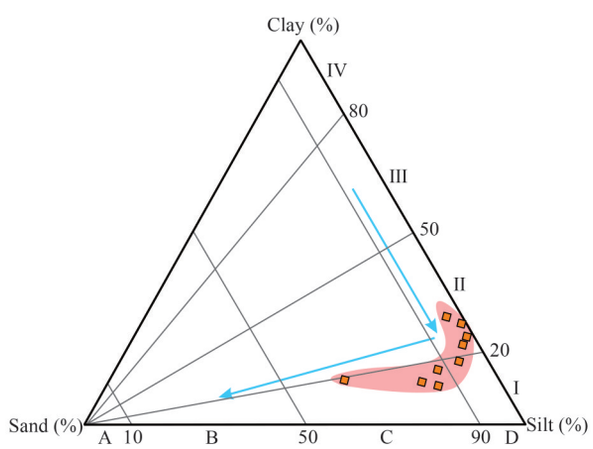

Fig.6 The Pejrup ternary diagram for the classification of the sedimentary dynamic of the sediment core in the Yongjiang River estuary

decreased and the hydrodynamic force weakened from direction A to D of the diagram. Grain sizes became finer from direction I to IV, indicating weakening of the hydrodynamic force and low disturbance of the water medium. The sediments of the Yongjiang River estuary are distributed in the C-I area on the Pejrup diagram for the 8.9–6.9 m section, in the D-I and D-II areas for the 6.9–3.9 m section, and in the C-II and D-I areas for the 3.9–0 m section (Fig.6). These reflect the changing course of hydrodynamic conditions from strong (8.9–6.9 m) to weak (6.9–3.9 m) to strong (3.9–0 m) along the core profile, thus proving that the energy of the sedimentary environment changed from relatively high to low and then to high. Similarly, Zhao et al. (2018a) studied the sediment core H5 of the Changjiang River mouth (East China Sea) and found that the sediments were mainly clay and silt, and the contents of silt at the bottom were relatively more than the top, reflecting changes in the hydrodynamic condition from strong to weak and in the sedimentary environment from high to low energy.

4.2 Sources of sedimentary organic matter

In general, $\delta^{13}C$ values and TOC/TN ratios are both indicators to OM sources. Many macromolecular compounds of higher terrestrial plants, such as cellulose, hemicellulose, and lignin, do not contain nitrogen; hence, the TOC/TN ratio of terrestrial organic compounds is higher (>20) than that of marine organic compounds (~7), and soil TOC/TN molar ratios range from 8 to 12 (Hedges et al., 1997). Based on these ranges, the C/N ratios (from 8.00 to 12.14) in this study may be indicative of soil organic matter. $\delta^{13}C$ values generally distinguish between terrestrial C3 photosynthetic plants (-22‰ to -28‰) and C4 plants (-12‰ to -15‰; Meyers, 1994), and marine and estuarine phytoplankton have $\delta^{13}C$ values ranging from -19‰ to -21‰ (Fry and Sherr, 1989) and from -25‰ to -30‰ (Goñi et al., 2003), respectively. The $\delta^{13}C$ values (from -24.80‰ to -23.60‰) and C/N ratios (from 8.00 to 12.14) found in our study area indicate that terrigenous sources have made a relatively large contribution to the OM in the Yongjiang River estuary. A plot of the TN/TOC atomic ratios vs. $\delta^{13}C$ values showed the presence of C3 soil OM (Fig.7), and a plot of the Λ (mg/100-mg OC) vs. $\delta^{13}C$ values showed a large amount of soil-derived OM at the Yongjiang River estuary (Fig.8).

To perform a quantitative evaluation of the OM

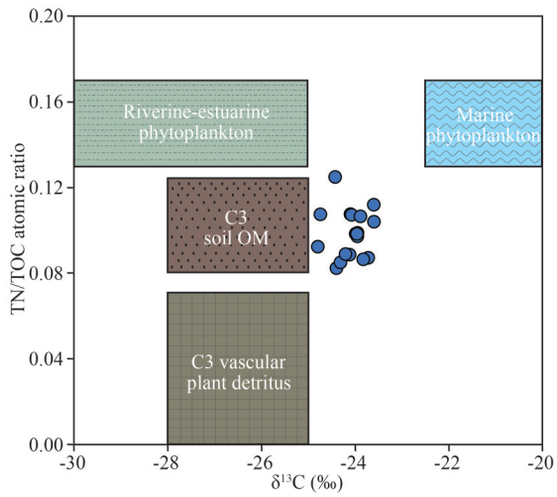

Fig.7 Plot of TN/TOC atomic ratios versus $\delta^{13}C$ values for sediments along the core in the Yongjiang River estuary

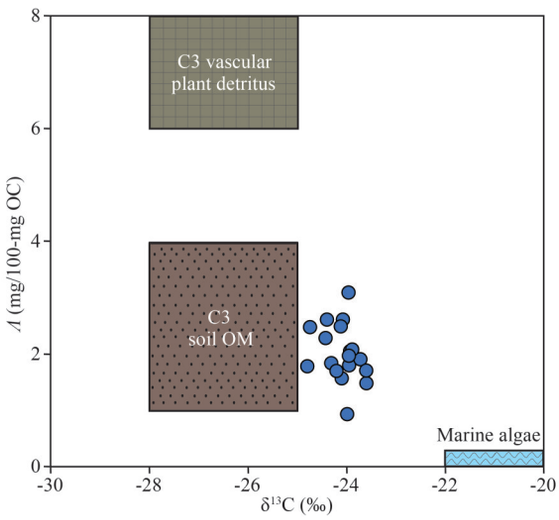

Fig.8 Plot of Λ (mg/100-mg OC) versus $\delta^{13}C$ values for sediments along the core in the Yongjiang River estuary

sources for the Yongjiang River estuary, the Shultz and Calder end-member mixing model (Shultz and Calder, 1976) was used to estimate the relative contribution of marine and terrestrial sources of the sedimentary OM. The relative contribution of terrestrial OC (f_T) was calculated as follows (Minoura et al., 1997):

$$f_T=(\delta^{13}C_{marine}-\delta^{13}C_{sediment})/(\delta^{13}C_{marine}-\delta^{13}C_{terrestrial}),$$

where the relative contribution of marine OC (f_M) is expressed as $f_M=1-f_T$. The $\delta^{13}C_{terrestrial}$ value used was -27.1‰, which was based on the end-member obtained by Wu et al. (2002) for terrestrial OM in

sediments of the Changjiang River. The $\delta^{13}C_{marine}$ value used was -19.5‰, which was based on the end-member obtained by Cai et al. (1992) for marine OM in sediments from the Changjiang River estuary. The variation in the trend of terrestrial OC (f_T) in terms of depth was similar to that of TOC (Fig.3), indicating that the source of OM in the sediment was greatly influenced by terrestrial OM. The f_T was 53.95%–69.68%, indicating that the sediments of the Yongjiang River estuary had a high contribution of terrestrial OM (>50%; Supplementary Table S2), which is comparable to the f_T range of 51.32%–63.16% in the salt marsh at the south side of Hangzhou Bay (Yuan et al., 2017). Terrestrial OM is the major component of the OM in the bulk sediments of the Yongjiang River estuary mainly because the estuary is situated nearshore, and the river delivers terrestrial OM to this location. In addition, this location is situated at the outlet of Hangzhou Bay, so these materials could be from the Changjiang River or Hangzhou Bay.

4.3 Vegetation source and diagenesis

Many studies conducted in Hangzhou Bay, the Qiantang River, the Changjiang River, and the East China Sea have found sediments S/V values greater than 0.6 and C/V values greater than 0.05, indicating the presence of nonwoody angiosperms in this region (Li et al., 2013, 2014; Wu et al., 2013; Xu et al., 2016; Yuan et al., 2017; Loh et al., 2018). The Yongjiang River estuary sediment core was found to have S/V ratios of 0.20–0.73, indicating the presence of angiosperm tissues, and C/V values of 0.03–0.19, indicating the predominance of nonwoody tissues. A plot of S/V vs. C/V (Fig.9) provided further evidence of the presence of nonwoody angiosperms, with a small contribution from woody angiosperms, near the Yongjiang River estuary. Thus, the estuary was found to have S/V and C/V ratios corresponding to those of the Changjiang River estuary and Hangzhou Bay.

Although lignin is typically stable, bacteria and fungi can degrade it to a certain extent under oxygen-rich conditions (Hedges and Mann, 1979). The Yongjiang River estuary sediments were found to have a wide range of $(Ad/Al)_V$ values, from 0.32 to 1.57, indicating that most of the lignin in the sediments near the Yongjiang River estuary originated from plant debris that had undergone a medium to high degree of lignin degradation. Loh et al. (2018) compared lignin in the sediments of the Andong salt marsh of Hangzhou Bay (average $(Ad/Al)_V$=0.66), the Changjiang River estuary (average $(Ad/Al)_V$=0.18), and the Qiantang River (average $(Ad/Al)_V$=1.06) and found that the degree of lignin degradation was the lowest in the Changjiang River estuary and the highest in the Qiantang River. The degree of lignin degradation at the Yongjiang River estuary was higher than that of the Changjiang River estuary and Hangzhou Bay, indicating that our sampling location also received materials from the Changjiang River and adjacent sea areas and that these materials had undergone decomposition during transportation.

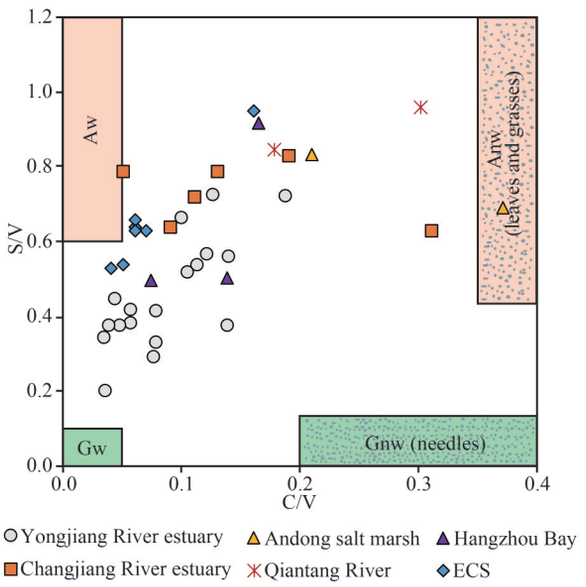

Fig.9 A plot of S/V vs. C/V for the sediments in the Yongjiang River estuary and its surrounding basins

Aw: woody angiosperm plants; Anw: nonwoody angiosperm plants; Gw: woody gymnosperm plants; Gnw: nonwoody gymnosperm plants. Data source: Andong salt marsh (Yuan et al., 2017), Hangzhou Bay (Xu et al., 2016), Qiantang River (Yuan et al., 2017), Changjiang River estuary (Li et al., 2014; Xu et al., 2016), and ECS (Li et al., 2013).

4.4 Significance of rare earth elements

REEs in sedimentary environments are mainly controlled by parent rocks and are often used as tracers to reflect the provenance of sediments (Rollinson, 1993; Zhai et al., 2018; Zhao et al., 2018b; Wang et al., 2020). REEs do not easily migrate during the weathering, transportation, and supergene geological processes of parent rocks and are generally considered to originate mainly from continental sources (Rollinson, 1993). Thus, the contents and distributions of ΣREEs and LREE/HREE ratios in sediments are useful in determining the provinance (Liu et al., 2015; Jung et al., 2021).

Nevertheless, the LREE/HREE ratios should be interpreted with caution. Large LREE/HREE ratios in sediment (LREE/HREE>0) indicate enriched LREE, reflecting a terrigenous source (Minai et al., 1992; Zhao et al., 2021). The LREE/HREE ratios of the Yongjiang River estuary ranged from 8.34 to 8.92, indicating a terrestrial source.

The REE compositions of sediments from Hangzhou Bay (unpublished data), the Changjiang River (Yang and Li, 1999), the Huanghe (Yellow) River (Yang and Li, 1999), the East China Sea (Zhao et al., 1990), Chinese loess (Wen et al., 1981), oceanic crust (Wen et al., 1981), and continental crust (Wen et al., 1981) were normalized to the North American shales (NASC) (Haskin et al., 1968) and are shown in Fig.10. The normalized REE distribution of the Yongjiang River estuary sediment core samples to NASC at different depths showed similar patterns, implying uniformity of source rocks during sedimentary transport and deposition (McLennan, 1989; Wang et al., 2020). Similarly, the NASC-normalized REE distribution patterns of the core exhibited patterns similar to those of the Changjiang River, the Huanghe River, and Chinese loess, indicating the predominance of terrestrial REE sources. The distribution curve of the sediment core of the Yongjiang River estuary was very close to those of Hangzhou Bay and the Changjiang River, indicating that the sediment source was affected by material from these two water bodies (Fig.10).

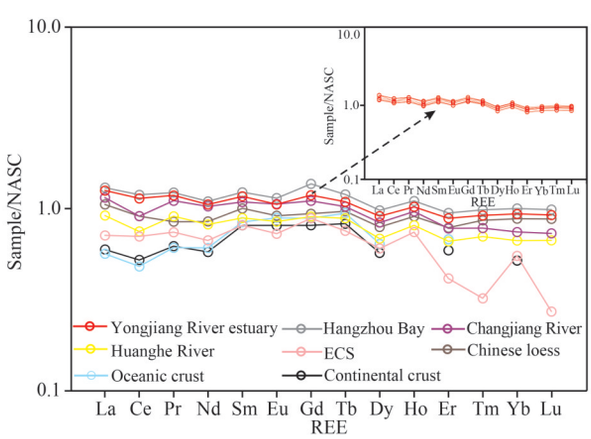

Fig.10 North American shales (NASC)-normalized REE patterns from nearby study areas and potential sediment sources

Data sources: Hangzhou Bay (unpublished data), Changjiang River (Yang and Li, 1999), Huanghe River (Yang and Li, 1999), East China Sea (Zhao et al., 1990), Chinese loess (Wen et al., 1981), oceanic crust (Wen et al., 1981), continental crust (Wen et al., 1981).

4.5 Environmental change at the Yongjiang River estuary

Climate and environmental changes in central and eastern China mainly include sea-level rise, seawater intrusion, and changes in temperature and hydrodynamic conditions (Easterling et al., 2000; Wu and Liu, 2004). Several studies worldwide have found indications of a cold period ca. 14 000 a BP. For example, pollen and charcoal records from Lake Sentarum in West Kalimantan of Indonesia showed the predominance of montane-submontane taxa during the Late Pleistocene and the Last Glacial Maximum, indicating a lowering of the temperature during this time (Anshari et al., 2001). A study on Chihuahuenos Bog in southwest of North America found that deglaciation occurred from ca. 14 100 to 14 000 a BP, during which the period before 14 000 a BP was rather unproductive (less vegetated) but in a transition to spruce parkland initiated after 14 000 a BP (Anderson et al., 2008a, b). The low Λ values detected in the sediments at the Yongjiang River estuary from ca. 14 500 and ca. 13 900 a BP indicate a low abundance of vegetation at the time, which could be attributed to the cold temperatures. Low S/V and C/V ratios during this time indicate the presence of woody gymnosperm tissues. This is consistent with a study by Lin et al. (2017) in which a predominance of woody gymnosperms *Pinus* and *Quercus* in the southern part of Hangzhou Bay from ca. 15 000 a BP to 14 000 a BP was found.

The period from ca. 15 000 a BP to ca. 8 800 a BP was characterized by increases in temperature and sea level (Wang and Wang, 1980; Hou and Fang, 2011). Another study found the Linxia Basin (Gansu, NW China) at the northeast margin of the Tibetan Plateau was characterized by dry and wet conditions from ca. 13 100 a BP to ca. 8 000 a BP (Fan et al., 2007), which explained the overall increase in Λ values in the Yongjiang River estuary sediment core from ca. 14 000 a BP to ca. 11 000 a BP, and indicated that increased temperature played an important role in the greater vegetation abundance in the watershed surrounding this area. Increased S/V and C/V ratios during this time span indicate an increasing abundance of nonwoody angiosperm tissues. This explanation is consistent with Lin et al. (2017) in which the types of vegetation in the southern bank of Hangzhou Bay from ca. 14 000 a BP to 11 000 a BP were found mainly woody angiosperm tissues, including Poaceae and Chenopodiaceae.

During the latest Pleistocene and earliest Holocene, there was a first abrupt warm period of the last deglaciation happening during the Bølling-Allerød (B-A) interstadial (ca. 14 600–12 900 a BP), which was identified in many archives and related to the strengthening of the Atlantic Meridional Overturing Circulation (Moreno et al., 2010; Naughton et al., 2016). In our study, this period was characterized by high TOC contents and low $\delta^{13}C$ values, as well as high Λ values after some time lag (Fig.11), suggesting that a lag in enhanced growth of vegetation and increased terrestrial runoff. Previous studies have found time lag effects on vegetation abundance caused by variation in temperature because plant growth has a time lag in responses to temperature change (Piao et al., 2003, 2004). Hence, the highest Λ value detected in the core taken from the Yongjiang River estuary at ca. 11 000 a BP was most likely a response to the higher temperatures in the preceding years, namely the B-A warm period. The Younger Dryas (YD) event between ca. 12 900 a BP and ca. 11 500 a BP was an abrupt cooling event that interrupted the deglacial warming trend in association with weakening of the Atlantic Meridional Overturing Circulation after the B-A warm event (Wang and Wang, 1980; Hou and Fang, 2011; Renssen et al., 2018). During YD period, there TOC content was low and $\delta^{13}C$ value was high, indicating a decreased plant growth rate and lower terrestrial runoff. The YD event could have caused the low Λ values near the Yongjiang River estuary found around 10 500 a BP, which shows again a time lag response of vegetation abundance to temperature variation, and also be seen on several other occasions along the sediment core in the Yongjiang River estuary. Therefore, the B-A and YD periods had a great influence on the changes of vegetation environment. Similarly, Hong et al. (2014) reconstructed the Indian summer monsoon (ISM) using a 15 000-year plant cellulose $\delta^{13}C$ proxy record from the Yuexi peat bog (Sichuan, SW China), and found that the ISM decreased abruptly during the YD period and increased abruptly during the B-A period.

The Holocene was characterized by higher temperatures than the Late Pleistocene. A study of sediment cores from the Song Hong delta, Vietnam, revealed that the period from ca. 10 470 a BP to ca. 5 340 a BP was characterized by a warm and wet climate with short cooling periods (Li et al., 2006). The mid-Holocene from ca. 8 800 a BP to ca. 4 200 a BP was characteristic of higher temperatures than modern times' and was considered the warmest period of the Holocene in the eastern China (Wang and Wang, 1980; Hou and Fang, 2011). However, the higher temperatures during early and mid-Holocene compared to the Late Pleistocene did not result in the increase in Λ values in the Yongjiang River estuary before ca. 11 000 a BP, which could be due to the already stable environment in this period.

The sediment core in the Yongjiang River estuary showed that Λ values was decreased in the period from ca. 3 550 a BP to ca. 680 a BP. The 4.2-ka event was an abrupt event of the Holocene and was characteristic of dry and cool climates in the world. This event is believed having played a major role in the collapse of major ancient civilizations (Ran et al., 2019), such as the Chinese Neolithic culture

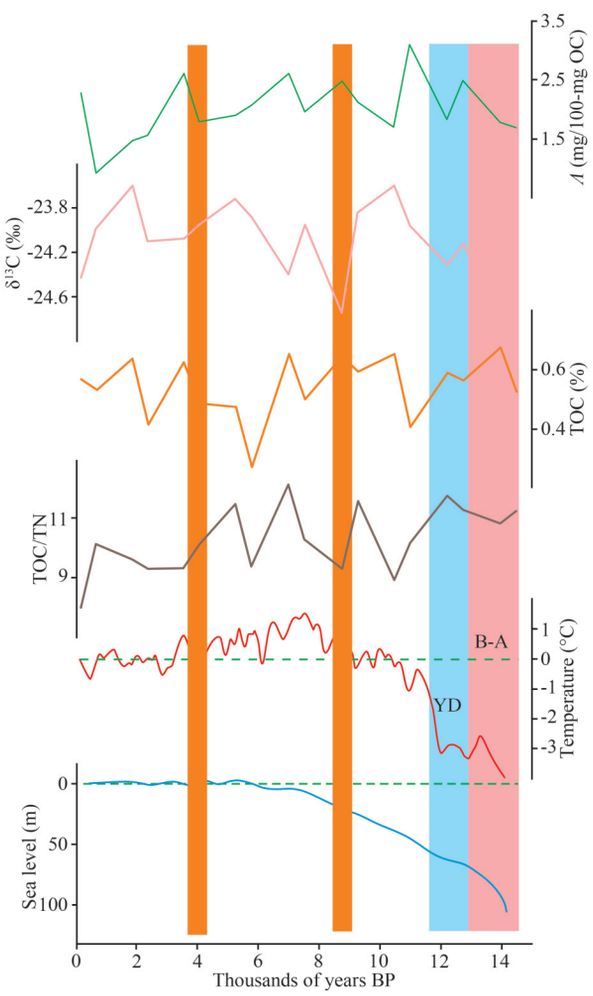

Fig.11 Diagram of temperature (extracted from Hou and Fang (2011), sea level TOC/TN, TOC, $\delta^{13}C$, and Λ changes over time

B-A: Bølling-Allerød; YD: Younger Dryas.

(including the Liangzhu Culture), which was declined at ca. 4 000 a BP. During this period, the climate in China was dominated primarily by cooling and precipitation fluctuations, and human activities were restricted (Wang et al., 2004; Wu and Liu, 2004), which could have been the cause of the low Λ values in this period as revealed in the Yongjiang River estuary core. On the other hand, our results show an increase in terrestrial OM since ca. 500 a BP, which is consistent with the results of other studies done in nearby regions. The population increased in south of the Changjiang River, and human activity was relatively intense after 800 a BP, delivering more soil-derived OM into the estuary (Li et al., 2016; Wang et al., 2018). For example, Li et al. (2016) found evidence that the population of the Changjiang River basin was increased nearly tenfold after 800 a BP, thus affecting the amount of terrestrial OM input to the estuary. The overall gradual increase of TOC from ca. 6 000 a BP to the top of the core (in the modern time) was mainly influenced by hydrodynamic sorting processes driven by climate factors. The warm and humid climate conditions during this period were dominated by fine-grained sediments, and the hydrodynamic conditions for the accumulation of TOC were relatively stable (Wan et al., 2007; Zhao et al., 2018c).

5 CONCLUSION

A sediment core collected from the southern outlet of the Hangzhou Bay in the Yongjiang River estuary was analyzed on grain size, lignin, bulk elemental composition, stable carbon isotopes, and REEs. Based on the vertical distribution of these parameters, we drew the following conclusions:

(1) The grain size characteristics of the core can be divided into sections from the bottom to the top, showing silt from 8.9 to 3.9 m and clayey silt from 3.9 m to the top of the core, indicating that the hydrodynamic conditions became weaker over time.

(2) The $\delta^{13}C$ values (-24.88‰–-24.43‰), Λ values (0.93–3.09 mg/100-mg OC), C/N molar ratios (8.00–12.14), and LREE/HREE ratios (8.34–8.92) indicate a predominance of terrestrial sources of sediments in the Yongjiang River estuary, mainly coming from the Changjiang River.

(3) The vegetation sources of the lignin in the sediments were determined using the lignin characteristic parameters S/V (0.42–0.73) and C/V (0.03–0.19), which indicate a predominance of nonwoody angiosperms. The terrestrial OM underwent a medium to high degree of degradation, as indicated by $(Ad/Al)_V$ values (0.32–1.57).

(4) Total lignin, Λ, had a relatively good response to temperature changes that began in the Late Pleistocene. High and stable lignin content corresponded to the warm Holocene period from ca. 8 500 a BP to ca. 4 500 a BP. However, extreme climate changes, such as the Bøllinge-Allerød interstadial and the Younger Dryas stadial, changed the Λ values. The changes in Λ values reflect the response of terrestrial vegetation to climate change and reveal that the temperature change had a time lag effect on vegetation abundance. Thus, lignin records were able to accurately reflect environmental changes in the Yongjiang River estuary since the Late Pleistocene. In addition, an increase in Λ values at the top of the sediment core was due to increasing human activity since ca. 500 a BP.

6 DATA AVAILABILITY STATEMENT

All data generated and/or analyzed during this study are included in this manuscript or in the supplementary materials.

7 ACKNOWLEDGMENT

We would like to thank the East China Survey and Design Institute for support in sampling matters and Chuan LI and Tao WU, Ocean College, Zhejiang University, for their assistance with laboratory and data analyses.

References

Anderson R S, Allen C D, Toney J L et al. 2008a. Holocene vegetation and fire regimes in subalpine and mixed conifer forests, southern Rocky Mountains, USA. *International Journal of Wildland Fire*, **17**(1): 96-114, https://doi.org/10.1071/WF07028.

Anderson R S, Jass R B, Toney J L et al. 2008b. Development of the mixed conifer forest in northern New Mexico and its relationship to Holocene environmental change. *Quaternary Research*, **69**(2): 263-275, https://doi.org/10.1016/j.yqres.2007.12.002.

Anshari G, Kershaw A P, van der Kaars S. 2001. A Late Pleistocene and Holocene pollen and charcoal record from peat swamp forest, Lake Sentarum Wildlife Reserve, West Kalimantan, Indonesia. *Palaeogeography, Palaeoclimatology, Palaeoecology*, **171**(3-4): 213-228, https://doi.org/10.1016/S0031-0182(01)00246-2.

Boutton T W. 1991. Stable carbon isotope ratios of natural materials: I. Sample preparation and mass spectrometric analysis. *In*: Coleman D C, Fry B eds. Carbon Isotope Techniques. Academic Press, San Diego. p.155-171, https://doi.org/10.1016/B978-0-12-179730-0.50015-1.

Cai D L, Tan F C, Edmond J M. 1992. Organic carbon isotope geochemistry of the Changjiang (Yangtze River) Estuary. *Geochimica*, (3): 305-312, https://doi.org/10.19700/j.0379-1726.1992.03.012. (in Chinese with English abstract)

Chang Y P, Wang W L, Chen M T. 2009. The last 100 000 years' palaeoenvironmental changes inferred from the diatom assemblages of core MD012404 from the Okinawa Trough, East China Sea. *Journal of Quaternary Science*, **24**(8): 890-901, https://doi.org/10.1002/jqs.1316.

Chen C Z, Chen L, Li F P et al. 2019. Urgent caution to trace organometal pollution: occurrence, distribution and sources of methyltins, butyltins and phenyltins in sediments from South Hangzhou Bay, China. *Environmental Pollution*, **246**: 571-577, https://doi.org/10.1016/j.envpol.2018.12.037.

Easterling D R, Meehl G A, Parmesan C et al. 2000. Climate extremes: observations, modeling, and impacts. *Science*, **289**(5487): 2068-2074, https://doi.org/10.1126/science.289.5487.2068.

Fan M J, Dettman D L, Song C H et al. 2007. Climatic variation in the Linxia basin, NE Tibetan Plateau, from 13.1 to 4.3 Ma: the stable isotope record. *Palaeogeography, Palaeoclimatology, Palaeoecology*, **247**(3-4): 313-328, https://doi.org/10.1016/j.palaeo.2006.11.001.

Folk R L, Andrews P B, Lewis D W. 1970. Detrital sedimentary rock classification and nomenclature for use in New Zealand. *New Zealand Journal of Geology and Geophysics*, **13**(4): 937-968, https://doi.org/10.1080/00288306.1970.10418211.

Fry B, Sherr E B. 1989. δ13C measurements as indicators of carbon flow in marine and freshwater ecosystems. *In*: Stable Isotopes in Ecological Research. Springer, New York. p.196-229, https://doi.org/10.1007/978-1-4612-3498-2_12.

Gong F, Hao T, Liu Y et al. 2017. Evidence for paleoclimate changes from lignin records of sediment core A02 in the southern Yellow Sea since ~9.5 cal. kyr B. P. *Palaeogeography, Palaeoclimatology, Palaeoecology*, **479**: 173-184, https://doi.org/10.1016/j.palaeo.2017.05.014.

Goñi M A, Hedges J I. 1992. Lignin dimers: structures, distribution, and potential geochemical applications. *Geochimica et Cosmochimica Acta*, **56**(11): 4025-4043, https://doi.org/10.1016/0016-7037(92)90014-A.

Goñi M A, Teixeira M J, Perkey D W. 2003. Sources and distribution of organic matter in a river-dominated estuary (Winyah Bay, SC, USA). *Estuarine, Coastal and Shelf Science*, **57**(5-6): 1023-1048, https://doi.org/10.1016/S0272-7714(03)00008-8.

Goñi M A, Yunker M B, Macdonald R W et al. 2000. Distribution and sources of organic biomarkers in arctic sediments from the Mackenzie River and Beaufort Shelf. *Marine Chemistry*, **71**(1-2): 23-51, https://doi.org/10.1016/S0304-4203(00)00037-2.

Haskin L A, Haskin M A, Frey F A et al. 1968. Relative and absolute terrestrial abundances of the rare earths. *In*: Ahrens L H ed. Origin and Distribution of the Elements. Pergamon, Oxford. p.889-912, https://doi.org/10.1016/B978-0-08-012835-1.50074-X.

Hedges J I, Ertel J R, Leopold E B. 1982. Lignin geochemistry of a Late Quaternary sediment core from Lake Washington. *Geochimica et Cosmochimica Acta*, **46**(10): 1869-1877, https://doi.org/10.1016/0016-7037(82)90125-9.

Hedges J I, Keil R G, Benner R. 1997. What happens to terrestrial organic matter in the ocean? *Organic Geochemistry*, **27**(5-6): 195-212, https://doi.org/10.1016/S0146-6380(97)00066-1.

Hedges J I, Mann D C. 1979. The characterization of plant tissues by their lignin oxidation products. *Geochimica et Cosmochimica Acta*, **43**(11): 1803-1807, https://doi.org/10.1016/0016-7037(79)90028-0.

Hedges J I, Parker P L. 1976. Land-derived organic matter in surface sediments from the Gulf of Mexico. *Geochimica et Cosmochimica Acta*, **40**(9): 1019-1029, https://doi.org/10.1016/0016-7037(76)90044-2.

Hong B, Hong Y T, Uchida M et al. 2014. Abrupt variations of Indian and East Asian summer monsoons during the last deglacial stadial and interstadial. *Quaternary Science Reviews*, **97**: 58-70, https://doi.org/10.1016/j.quascirev.2014.05.006.

Hou G L, Fang X Q. 2011. Characteristics of Holocene temperature change in China. *Progress in Geography*, **30**(9): 1075-1080, https://doi.org/10.11820/dlkxjz.2011.09.001. (in Chinese with English Abstract)

Hu F S, Hedges J I, Gordon E S et al. 1999. Lignin biomarkers and pollen in postglacial sediments of an Alaskan lake. *Geochimica et Cosmochimica Acta*, **63**(9): 1421-1430, https://doi.org/10.1016/S0016-7037(99)00100-3.

Jex C N, Pate G H, Blyth A J et al. 2014. Lignin biogeochemistry: from modern processes to Quaternary archives. *Quaternary Science Reviews*, **87**: 46-59, https://doi.org/10.1016/j.quascirev.2013.12.028.

Jung H S, Kim J, Lim D et al. 2021. REE fractionation and quantification of sediment source in the Yellow Sea mud deposits, East Asian marginal sea. *Continental Shelf Research*, **217**: 104374, https://doi.org/10.1016/j.csr.2021.104374.

Kawahata H, Ohshima H. 2004. Vegetation and environmental record in the northern East China Sea during the late Pleistocene. *Global & Planetary Change*, **41**(3-4): 251-273, https://doi.org/10.1016/j.gloplacha.2004.01.011.

Kuai Y, Tao J F, Zhang Q et al. 2017. Numerical simulation on the tidal current and sediment for the Yongjiang River and out sea area. *Port & Waterway Engineering*, (7): 58-67, https://doi.org/10.3969/j.issn.1002-4972.2017.07.013. (in Chinese with English abstract)

Li D, Yao P, Bianchi T S et al. 2014. Organic carbon cycling in sediments of the Changjiang Estuary and adjacent shelf: implication for the influence of Three Gorges Dam. *Journal of Marine Systems*, **139**: 409-419, https://doi.org/10.1016/j.jmarsys.2014.08.009.

Li F P, Mao L C, Jia Y B et al. 2018. Distribution and risk assessment of trace metals in sediments from Yangtze River estuary and Hangzhou Bay, China. *Environmental Science and Pollution Research*, **25**(1): 855-866, https://

doi.org/10.1007/s11356-017-0425-0.

Li X X, Bianchi T S, Allison M A et al. 2013. Historical reconstruction of organic carbon decay and preservation in sediments on the East China Sea shelf. *Journal of Geophysical Research*: *Biogeosciences*, **118**(3): 1079-1093, https://doi.org/10.1002/jgrg.20079.

Li Z, Saito Y, Matsumoto E et al. 2006. Climate change and human impact on the Song Hong (Red River) Delta, Vietnam, during the Holocene. *Quaternary International*, **144**(1): 4-28, https://doi.org/10.1016/j.quaint.2005.05.008.

Li Z Q, Wu Y, Liu S M et al. 2016. An 800-year record of terrestrial organic matter from the East China Sea shelf break: links to climate change and human activity in the Changjiang Basin. *Deep Sea Research Part II*: *Topical Studies in Oceanography*, **124**: 64-73, https://doi.org/10.1016/j.dsr2.2015.01.006.

Lin Q L, Lin N, Ma H J. 2017. Late Quaternary sediments and paleoenvironmental evolution in Cixi, Hangzhou Bay south coast area. *Science Technology and Engineering*, **17**(9): 1-8, https://doi.org/10.3969/j.issn.1671-1815.2017.09.001. (in Chinese with English abstract)

Liu F W, Miao L, Cai G Q et al. 2015. The rare earth element geochemistry of surface sediments in four transects in the South China Sea and its geological significance. *Environmental Earth Sciences*, **74**(3): 2511-2522, https://doi.org/10.1007/s12665-015-4265-2.

Liu J Q, Cao K, Yin P et al. 2018a. The sources and transport patterns of modern sediments in Hangzhou Bay: evidence from clay minerals. *Journal of Ocean University of China*, **17**(6): 1352-1360, https://doi.org/10.1007/s11802-018-3710-8.

Liu Y, Deng L J, He J et al. 2020. Early to middle Holocene rice cultivation in response to coastal environmental transitions along the South Hangzhou Bay of eastern China. *Palaeogeography*, *Palaeoclimatology*, *Palaeoecology*, **555**: 109872, https://doi.org/10.1016/j.palaeo.2020.109872.

Liu Y, Ma C Y, Fan D D et al. 2018b. The Holocene environmental evolution of the inner Hangzhou Bay and its significance. *Journal of Ocean University of China*, **17**(6): 1301-1308, https://doi.org/10.1007/s11802-018-3562-2.

Loh P S, Cheng L X, Yuan H W et al. 2018. Impacts of human activity and extreme weather events on sedimentary organic matter in the Andong salt marsh, Hangzhou Bay, China. *Continental Shelf Research*, **154**: 55-64, https://doi.org/10.1016/j.csr.2018.01.005.

Loh P S, Reeves A D, Harvey S M et al. 2008. The fate of terrestrial organic matter in two Scottish sea lochs. *Estuarine*, *Coastal and Shelf Science*, **76**(3): 566-579, https://doi.org/10.1016/j.ecss.2007.07.023.

McLaren P, Bowles D. 1985. The effects of sediment transport on grain-size distributions. *SEPM Journal of Sedimentary Research*, **55**(4): 457-470, https://doi.org/10.1306/212F86FC-2B24-11D7-8648000102C1865D.

McLennan S M. 1989. Rare earth elements in sedimentary rocks: influence of provenance and sedimentary processes. *Reviews in Mineralogy and Geochemistry*, **21**(1): 169-200.

Meyers P A. 1994. Preservation of elemental and isotopic source identification of sedimentary organic matter. *Chemical Geology*, **114**(3-4): 289-302, https://doi.org/10.1016/0009-2541(94)90059-0.

Minai Y, Matsumoto R, Watanabe Y et al. 1992. Geochemistry of rare earth element and other trace elements in sediments from sites 798 end 799, Japan Sea. In: Proceeding of the Ocean Drilling Program, Scientific Results. Ocean Drilling Program, College Station, TX. p.719-737, http://doi.org/10.2973/odp.proc.sr.127128-1.180.1992.

Minoura K, Hoshino K, Nakamura T et al. 1997. Late Pleistocene-Holocene paleoproductivity circulation in the Japan Sea: sea-level control on $\delta^{13}C$ and $\delta^{15}N$ records of sediment organic material. *Palaeogeography*, *Palaeoclimatology*, *Palaeoecology*, **135**(1-4): 41-50, http://doi.org/10.1016/s0031-0182(97)00026-6.

Moreno A, Stoll H, Jiménez-Sánchez M et al. 2010. A speleothem record of glacial (25-11.6 kyr BP) rapid climatic changes from northern Iberian Peninsula. *Global and Planetary Change*, **71**(3-4): 218-231, https://doi.org/10.1016/j.gloplacha.2009.10.002.

Naughton F, Goñi M F S, Rodrigues T et al. 2016. Climate variability across the last deglaciation in NW Iberia and its margin. *Quaternary International*, **414**: 9-22, https://doi.org/10.1016/j.quaint.2015.08.073.

Onstad G D, Canfield D E, Quay P D et al. 2000. Sources of particulate organic matter in rivers from the continental USA: lignin phenol and stable carbon isotope compositions. *Geochimica et Cosmochimica Acta*, **64**(20): 3539-3546, https://doi.org/10.1016/S0016-7037(00)00451-8.

Orem W H, Colman S M, Lerch H E. 1997. Lignin phenols in sediments of Lake Baikal, Siberia: application to paleoenvironmental studies. *Organic Geochemistry*, **27**(3-4): 153-172, https://doi.org/10.1016/S0146-6380(97)00079-X.

Pang H J, Lyu S S, Chen X G et al. 2017. Heavy metal distribution and accumulation in the *Spartina alterniflora* from the Andong tidal flat, Hangzhou Bay, China. *Environmental Earth Sciences*, **76**(17): 627, https://doi.org/10.1007/s12665-017-6948-3.

Pejrup M. 1988. The triangular diagram used for classification of estuarine sediments: a new approach. *In*: De Boer P L, Van Gelder A, Nio S D eds. Tide-Influenced Sedimentary Environments and Facies. D. Reidel, Dordrecht. p.298-300.

Piao S L, Fang J Y, Ji W et al. 2004. Variation in a satellite-based vegetation index in relation to climate in China. *Journal of Vegetation Science*, **15**(2): 219-226, https://doi.org/10.1658/1100-9233(2004)015[0219:VIASVI]2.0.CO;2.

Piao S L, Fang J Y, Zhou L M et al. 2003. Interannual variations of monthly and seasonal normalized difference vegetation index (NDVI) in China from 1982 to 1999. *Journal of Geophysical Research*: *Atmospheres*, **108**(D14): 4401, https://doi.org/10.1029/2002JD002848.

Ran M, Chen L. 2019. The 4.2 ka BP climatic event and its cultural responses. *Quaternary International*, **521**: 158-

167, https://doi.org/10.1016/j.quaint.2019.05.030.

Renssen H, Goosse H, Roche D M et al. 2018. The global hydroclimate response during the Younger Dryas event. *Quaternary Science Reviews*, **193**: 84-97, https://doi.org/10.1016/j.quascirev.2018.05.033.

Rollinson H R. 1993. Using Geochemical Data: Evaluation, Presentation, Interpretation. Routledge, London. 384p. https://doi.org/10.4324/9781315845548.

Shultz D J, Calder J A. 1976. Organic carbon $^{13}C^{12}C$ variations in estuarine sediments. *Geochimica et Cosmochimica Acta*, **40**(4): 381-385, https://doi.org/10.1016/0016-7037(76)90002-8.

Song Z K, Shi W Y, Zhang J B et al. 2020. Transport mechanism of suspended sediments and migration trends of sediments in the central Hangzhou Bay. *Water*, **12**(8): 2189, https://doi.org/10.3390/w12082189.

Su J L, Wang K S. 1989. Changjiang river plume and suspended sediment transport in Hangzhou Bay. *Continental Shelf Research*, **9**(1): 93-111, https://doi.org/10.1016/0278-4343(89)90085-X.

Tareq S M, Kitagawa H, Ohta K. 2011. Lignin biomarker and isotopic records of paleovegetation and climate changes from Lake Erhai, southwest China, since 18.5 ka BP. *Quaternary International*, **229**(1-2): 47-56, https://doi.org/10.1016/j.quaint.2010.04.014.

Tesi T, Miserocchi S, Goñi M A et al. 2007. Organic matter origin and distribution in suspended particulate materials and surficial sediments from the western Adriatic Sea (Italy). *Estuarine*, *Coastal and Shelf Science*, **73**(3-4): 431-446, https://doi.org/10.1016/j.ecss.2007.02.008.

Wan S M, Li A C, Clift P D et al. 2007. Development of the East Asian monsoon: mineralogical and sedimentologic records in the northern South China Sea since 20 Ma. *Palaeogeography*, *Palaeoclimatology*, *Palaeoecology*, **254**(3-4): 561-582, https://doi.org/10.1016/j.palaeo.2007.07.009.

Wang G, Wang Y L, Wei Z F et al. 2020. Geochemical records of Qionghai Lake sediments in southwestern China linked to late Quaternary climate changes. *Palaeogeography*, *Palaeoclimatology*, *Palaeoecology*, **560**: 109902, https://doi.org/10.1016/j.palaeo.2020.109902.

Wang J P, Yao P, Bianchi T S et al. 2015. The effect of particle density on the sources, distribution, and degradation of sedimentary organic carbon in the Changjiang Estuary and adjacent shelf. *Chemical Geology*, **402**: 52-67, https://doi.org/10.1016/j.chemgeo.2015.02.040.

Wang J T, Wang P X. 1980. Relationship between sea-level changes and climatic fluctuations in East China since late Pleistocene. *Acta Geographica Sinica*, **35**(4): 299-312, https://doi.org/10.11821/xb198004003. (in Chinese with English abstract)

Wang Q, Yang S Y. 2013. Clay mineralogy indicates the Holocene monsoon climate in the Changjiang (Yangtze River) Catchment, China. *Applied Clay Science*, **74**: 28-36, https://doi.org/10.1016/j.clay.2012.08.011.

Wang S W, Zhou T J, Cai J N et al. 2004. Abrupt climate change around 4 ka BP: role of the thermohaline circulation as indicated by a GCM experiment. *Advances in Atmospheric Sciences*, **21**(2): 291-295, https://doi.org/10.1007/BF02915716.

Wang Z H, Saito Y, Zhan Q et al. 2018. Three-dimensional evolution of the Yangtze River mouth, China during the Holocene: impacts of sea level, climate and human activity. *Earth-Science Reviews*, **185**: 938-955, https://doi.org/10.1016/j.earscirev.2018.08.012.

Wen Q Z, Yu S H, Gu X F et al. 1981. A preliminary investigation of REE in loess. *Geochemistry*, (2): 151-157, https://doi.org/10.19700/j.0379-1726.1981.02.007. (in Chinese with English abstract)

Winterfeld M, Goñi M, Just J et al. 2015. Sources and age of terrigenous organic matter exported from the Lena River watershed, NE Siberia. *In*: Goldschmidt Conference. Prague.

Wu W X, Liu T S. 2004. Possible role of the "Holocene Event 3" on the collapse of Neolithic Cultures around the central plain of China. *Quaternary International*, **117**(1): 153-166, https://doi.org/10.1016/S1040-6182(03)00125-3.

Wu Y, Eglinton T, Yang L Y et al. 2013. Spatial variability in the abundance, composition, and age of organic matter in surficial sediments of the East China Sea. *Journal of Geophysical Research*: *Biogeosciences*, **118**(4): 1495-1507, https://doi.org/10.1002/2013JG002286.

Wu Y, Zhang J, Zhang Z F et al. 2002. Seasonal variability of stable carbon and nitrogen isotope of suspended particulate matter in the Changjiang River. *Oceanologia et Limnologia Sinica*, **33**(5): 546-552, https://doi.org/10.3321/j.issn:0029-814X.2002.05.012. (in Chinese with English abstract)

Xie D F, Pan C H, Wu X G et al. 2017. The variations of sediment transport patterns in the outer Changjiang Estuary and Hangzhou Bay over the last 30 years. *Journal of Geophysical Research*: *Oceans*, **122**(4): 2999-3020, https://doi.org/10.1002/2016JC012264.

Xing L, Zhang H L, Yuan Z N et al. 2011. Terrestrial and marine biomarker estimates of organic matter sources and distributions in surface sediments from the East China Sea shelf. *Continental Shelf Research*, **31**(10): 1106-1115, https://doi.org/10.1016/j.csr.2011.04.003.

Xu F L, Ji Z Q, Wang K et al. 2016. The distribution of sedimentary organic matter and implication of its transfer from Changjiang Estuary to Hangzhou Bay, China. *Open Journal of Marine Science*, **6**(1): 103-114, https://doi.org/10.4236/ojms.2016.61010.

Yang B J, Ljung K, Nielsen A B et al. 2021. Impacts of long-term land use on terrestrial organic matter input to lakes based on lignin phenols in sediment records from a Swedish forest lake. *Science of the Total Environment*, **774**: 145517, https://doi.org/10.1016/j.scitotenv.2021.145517.

Yang S Y, Li C X. 1999. Characteristic element compositions of the Yangtze and the Yellow River sediments and their geological background. *Marine Geology & Quaternary Geology*, **19**(2): 19-26, https://doi.org/10.1088/0256-307X/15/12/024. (in Chinese with English abstract)

Yuan H W, Chen J F, Ye Y et al. 2017. Sources and

distribution of sedimentary organic matter along the Andong salt marsh, Hangzhou Bay. *Journal of Marine Systems*, **174**: 78-88, https://doi.org/10.1016/j.jmarsys.2017.06.001.

Zhai L N, Wu C D, Ye Y T et al. 2018. Fluctuations in chemical weathering on the Yangtze Block during the Ediacaran-Cambrian transition: implications for paleoclimatic conditions and the marine carbon cycle. *Palaeogeography*, *Palaeoclimatology*, *Palaeoecology*, **490**: 280-292, https://doi.org/10.1016/j.palaeo.2017.11.006.

Zhang J, Wu Y, Jennerjahn T C et al. 2007. Distribution of organic matter in the Changjiang (Yangtze River) Estuary and their stable carbon and nitrogen isotopic ratios: implications for source discrimination and sedimentary dynamics. *Marine Chemistry*, **106**(1-2): 111-126, https://doi.org/10.1016/j.marchem.2007.02.003.

Zhang T, Li X G, Sun S W et al. 2013. Determination of lignin in marine sediment using alkaline cupric oxide oxidation-solid phase extraction-on-column derivatization-gas chromatography. *Journal of Ocean University of China*, **12**(1): 63-69, https://doi.org/10.1007/s11802-011-1936-z.

Zhang W Y, Jin H Y, Yao X Y et al. 2015. Grain size composition and transport of sedimentary organic carbon in the Changjiang River (Yangtze River) Estuary and Hangzhou Bay and their adjacent waters. *Acta Oceanologica Sinica*, **34**(10): 46-56, https://doi.org/10.1007/s13131-015-0711-y.

Zhao B C, Yan X X, Wang Z H et al. 2018a. Sedimentary evolution of the Yangtze River mouth (East China Sea) over the past 19,000 years, with emphasis on the Holocene variations in coastal currents. *Palaeogeography*, *Palaeoclimatology*, *Palaeoecology*, **490**: 431-449, https://doi.org/10.1016/j.palaeo.2017.11.023.

Zhao D B, Wan S M, Clift P D et al. 2018b. Provenance, sea-level and monsoon climate controls on silicate weathering of Yellow River sediment in the northern Okinawa Trough during late last glaciation. *Palaeogeography*, *Palaeoclimatology*, *Palaeoecology*, **490**: 227-239, https://doi.org/10.1016/j.palaeo.2017.11.002.

Zhao X, Wang S S, Pan C H et al. 2018c. Distribution characteristics and ecological risk assessment of nutrients in sediment particles in Hangzhou Bay, China. *IOP Conference Series*: *Earth and Environmental Science*, **191**: 012079, https://doi.org/10.1088/1755-1315/191/1/012079.

Zhao Y Y, Wang J T, Qin C Y et al. 1990. Rare-earth elements in continental shelf sediments of the China Seas. *Acta Sedimentologica Sinica*, **8**(1): 37-43, https://doi.org/CNKI:SUN:CJXB.0.1990-01-004. (in Chinese with English abstract)

Zhao Z Y, Wang H P, Zhao Z Z. 2021. Fractionation and provenances of rare earth elements in coastal sediments in tropical China. *Journal of Coastal Conservation*, **25**(1): 13, https://doi.org/10.1007/s11852-021-00803-w.

Zhu W J, Wang C, Hill J et al. 2018. A missing link in the estuarine nitrogen cycle? Coupled nitrification-denitrification mediated by suspended particulate matter. *Scientific Reports*, **8**(1): 2282, https://doi.org/10.1038/s41598-018-20688-4.

Electronic supplementary material

Supplementary material (Supplementary Tables S1–S4) is available in the online version of this article at https://doi.org/10.1007/s00343-023-2372-6.